Polymerization of Methyl Methacrylate Photoinitiated by 4,4′-Bis(*N,N*-diethylamino)benzophenone.
2. Oxygen Effects

V. D. McGinniss,*[1a] T. Provder, C. Kuo, and A. Gallopo[1b]

Glidden Coatings and Resins, Division of SCM Corporation,
Strongsville, Ohio 44136, and Montclair State College,
Upper Montclair, New Jersey. Received September 26, 1977

ABSTRACT: Polymerization of methyl methacrylate (MMA), in the presence of oxygen, photoinitiated by 4,4′-bis(*N,N*-diethylamino)benzophenone (DEABP) was shown to have a predictable induction period before initial steady rates of photopolymerization were obtained. This induction period is oxygen concentration dependent and the relative rates of change in oxygen concentration up to the induction period were found to depend on 0.548 order in initiator DEABP. Molecular weight distributions were found to be much broader in nitrogen–MMA photopolymerizations than in pure oxygen–MMA indicating a different efficient termination or photoinitiator (radical) quenching mechanism rather than complicated photoinitiator–photoproduct primary radical transfer to a growing polymer radical. The photoinitiator combinations of substituted aromatic carbonyl compounds (benzophenones and benzaldehydes) with DEABP showed increased reactivity (shorter induction periods) with electron withdrawing substituents rather than electron donating groups attached to the aromatic carbonyl compounds (longer induction periods) for the photopolymerization of MMA in air. Reaction mechanism and possible kinetic schemes, consistent with these experimental observations, are presented and discussed.

In our previous study, part 1, the basic kinetic analysis for polymerization of methyl methacrylate (MMA) with 4,4′-bis(*N,N*-diethylamino)benzophenone (DEABP) as the photoinitiator was discussed in detail.[2a] This section will examine some of the effects of oxygen on a photopolymerization system.

The interaction of oxygen in photopolymer systems is of extreme practical importance both in formation or degradation of the polymer.[2b] The ground state of oxygen is triplet in character and can react with a substrate by the following mechanism.[3–5]

1. Formation of ground-state charge-transfer complexes, such as styrene and oxygen, which upon absorption produce excited state complexes capable of initiating photopolymerization.

$$\mathrm{Sty} + \mathrm{O_2} \longrightarrow \underset{\text{ground state}}{[\mathrm{Sty}\text{- - -}\mathrm{O_2}]} \xrightarrow{h\nu} \tag{1}$$

$$\underset{\text{excited state}}{[\mathrm{Sty}\text{- - -}\mathrm{O_2}]^*} \longrightarrow \mathrm{P}\ \underset{\text{Sty}}{\mathrm{Sty}} \tag{2}$$

2. Formation of complexes with excited states of a sensitizer ("oxiplexes").

3. Quenching of excited electronic states of sensitizers (S), sometimes resulting in production of singlet oxygen ($^1\mathrm{O_2}$).

$$^1\mathrm{S} + {}^3\mathrm{O_2} \rightarrow \text{complex} \rightarrow {}^3\mathrm{S} + {}^3\mathrm{O_2} \tag{3}$$

$$^3\mathrm{S} + {}^3\mathrm{O_2} \rightarrow \text{complex} \rightarrow \mathrm{S} + {}^1\mathrm{O_2} \tag{4}$$

4. Direct interaction of a free-radical intermediate with oxygen.

$$\mathrm{S} \xrightarrow{h\nu} \mathrm{S}\cdot \quad \text{(photosensitizer radical formation)} \tag{5}$$

$$\mathrm{S}\cdot + \mathrm{O_2} \rightarrow \mathrm{SOO}\cdot \tag{6}$$

$$\mathrm{S}\cdot + \text{monomer [M]} \rightarrow \mathrm{S{-}M}\cdot \text{ (initiation)} \tag{7}$$

$$\mathrm{S{-}M}\cdot + \mathrm{O_2} \rightarrow \mathrm{S{-}MOO}\cdot \tag{8}$$

$$\mathrm{ROO}\cdot + \mathrm{RH} \rightarrow \mathrm{ROOH} + \mathrm{R}\cdot \tag{9}$$

The photochemistry associated with aromatic aminoketones is very sensitive to oxygen and the quantum yield for Michler's ketone (Mk) disappearance in cyclohexane has been shown to be critically dependent on the presence of oxygen.[6,7] For this reason we studied the photopolymerization of MMA in air using different concentrations of DEABP as photoinitiator.

Experimental Section

The experimental kinetic and molecular weight analysis techniques used in this work were previously described.[2a] Solutions were saturated with oxygen by bubbling air or pure oxygen into the dilatometer for 10 min and then sealing the reaction cell. Alternatively, initial photosensitizer concentrations with small amounts of monomer were added to the dilatometer and brought up to volume with saturated $\mathrm{N_2}$, air, or oxygen monomer solutions.

Results and Discussion

Induction Period. In Figure 1 is a plot of percent conversion vs. exposure time for the photopolymerization of MMA in the presence of air at different concentrations of DEABP. The linear portion of these curves was extrapolated to a time at 0% conversion. This extrapolated time value is defined as an induction period (τ) or the point at which a steady rate of conversion can be measured and is directly related to the photoinitiator concentration (DEABP) and the oxygen concentration dissolved in the monomer.[8]

The mechanism involved in achieving steady state monomer conversion after a decrease in oxygen concentration can be represented by the following reaction scheme:

$$\mathrm{DEABP} \xrightarrow{I_{\mathrm{abs}}\,\phi_{\mathrm{st}}} \mathrm{R}\cdot \quad I_{\mathrm{abs}}\phi_{\mathrm{st}} = I_{\mathrm{o}}\epsilon\phi_{\mathrm{st}}[\mathrm{DEABP}] \tag{10}$$

$$\mathrm{R}\cdot + \mathrm{M} \xrightarrow{K_1} \mathrm{M}\cdot \quad K_1[\mathrm{R}\cdot][\mathrm{M}] \tag{11}$$

$$\mathrm{R}\cdot + \mathrm{O_2} \xrightarrow{K_2} \mathrm{ROO}\cdot \quad K_2[\mathrm{R}\cdot][\mathrm{O_2}] \tag{12}$$

$$\mathrm{M}\cdot + \mathrm{M} \xrightarrow{K_3} \mathrm{P}\cdot \quad K_3[\mathrm{M}\cdot][\mathrm{M}] \tag{13}$$

$$\mathrm{P}\cdot + \mathrm{O_2} \xrightarrow{K_4} \mathrm{POO}\cdot \quad K_4[\mathrm{P}\cdot][\mathrm{O_2}] \tag{14}$$

In the initial stages of the photoreaction all processes are active. The decrease in the initial concentration of photoinitiator $[\mathrm{DEABP}]_i$ is represented by

$$\frac{\mathrm{d}[\mathrm{DEABP}]}{\mathrm{d}t} = -I_{\mathrm{o}}\epsilon\phi_{\mathrm{st}}[\mathrm{DEABP}]_i \tag{15}$$

0024-9297/78/2211-0405$01.00/0 1978 American Chemical Society

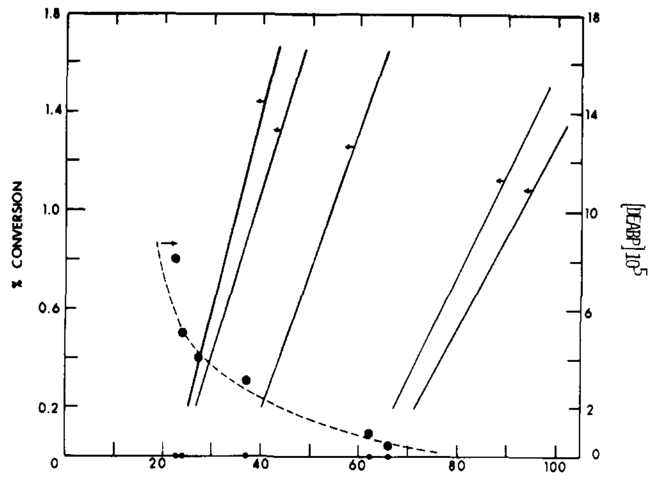

Figure 1. Photopolymerization of MMA in air at 30 °C with 4,4′-bis(diethylamino)benzophenone (DEABP) photoinitiator: (●) [DEABP] = 0.5, 1, 3, 4, 5, 8 × 10^{-5} M; (-●-) extrapolated induction period values.

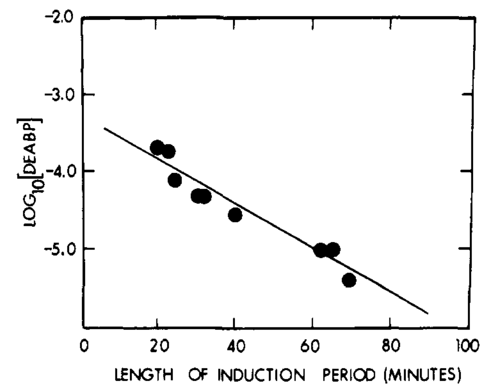

Figure 2. Log of [DEABP] vs. induction period (τ) (extrapolated values) for photopolymerization of MMA in air.

and

$$[\mathrm{DEABP}] = [\mathrm{DEABP}]_i e^{-I_0\epsilon\phi_{\mathrm{st}}\tau} \tag{16}$$

Thus

$$\log\,[\mathrm{DEABP}] = \tau I_0\epsilon\phi_{\mathrm{st}} \tag{17}$$

where τ is the exposure time to the end of the induction period.

A nonlinear plot of [DEABP] vs. τ is also shown in Figure 1 but can be linearized with a semilogarithmic plot as shown in Figure 2. The percent oxygen vs. induction period (Figure 3) is linear for a fixed concentration of DEABP (4 × 10^{-5} M) starting from a zero time of 13 min for all solutions (degassed or nitrogen sparged) up to pure oxygen. Similar linear plots for the photopolymerization of MMA in nitrogen and air at different DEABP concentrations normalized to the same zero time are shown in Figure 4. The slopes of these lines represent relative decreases in oxygen consumption as a function of exposure time ($-\mathrm{d}[\mathrm{O}_2]/\mathrm{d}t = \rho$) and photoinitiator concentrations.

Oxygen/Kinetic Effects. The relative rates of change in oxygen concentration can probably be represented by the following kinetic scheme:[9]

$$\mathrm{DEABP} \xrightarrow{I_{\mathrm{abs}}\phi_{\mathrm{st}}} \mathrm{R}\cdot \qquad I_{\mathrm{abs}}\phi_{\mathrm{st}} = I_0[\mathrm{DEABP}]\epsilon\phi_{\mathrm{st}} \tag{18}$$

$$\mathrm{R}\cdot + \mathrm{M} \xrightarrow{K_1} \mathrm{P}\cdot \qquad [\mathrm{R}\cdot][\mathrm{M}]K_1 \tag{19}$$

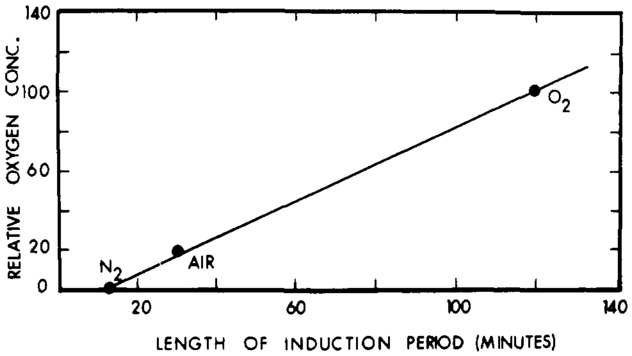

Figure 3. Percent oxygen vs. induction period (τ) for polymerization of MMA at a fixed [DEABP] = 4 × 10^{-5} M.

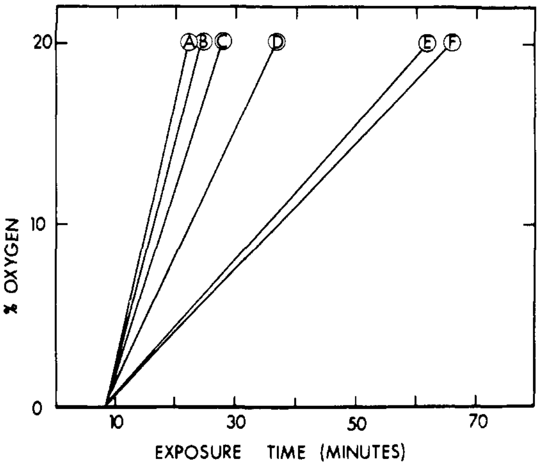

Figure 4. Percent oxygen vs. induction period for the photopolymerization of MMA in nitrogen and air normalized to zero time for [DEABP]: A = 8 × 10^{-5} M, B = 5 × 10^{-5} M, C = 4 × 10^{-5} M, D = 3 × 10^{-5} M, E = 1 × 10^{-5} M, F = 0.5 × 10^{-5} M.

$$\mathrm{R}\cdot + \mathrm{O}_2 \xrightarrow{K_2} \mathrm{ROO}\cdot \qquad [\mathrm{R}\cdot][\mathrm{O}_2]K_2 \tag{20}$$

$$\mathrm{P}\cdot + \mathrm{M} \xrightarrow{K_3} \mathrm{P}\cdot \qquad [\mathrm{P}\cdot][\mathrm{M}]K_3 = R_{\mathrm{p}} \tag{21}$$

$$\mathrm{P}\cdot + \mathrm{O}_2 \xrightarrow{K_4} \mathrm{POO}\cdot \qquad [\mathrm{P}\cdot][\mathrm{O}_2]K_4 \tag{22}$$

$$\left.\begin{array}{l} \mathrm{R}\cdot + \mathrm{R}\cdot \xrightarrow{K_5} \\ \mathrm{P}\cdot + \mathrm{P}\cdot \xrightarrow{K_6} \\ \mathrm{R}\cdot + \mathrm{RO}_2\cdot \xrightarrow{K_7} \\ \mathrm{P}\cdot + \mathrm{POO}\cdot \xrightarrow{K_8} \end{array}\right\} \text{termination} \quad \begin{array}{ll} 2[\mathrm{R}\cdot]^2K_5 & (23) \\ 2[\mathrm{P}\cdot]^2K_6 & (24) \\ [\mathrm{R}\cdot][\mathrm{RO}_2\cdot]K_7 & (25) \\ [\mathrm{P}\cdot][\mathrm{POO}\cdot]K_8 & (26) \end{array}$$

$$\mathrm{RO}_2\cdot + \mathrm{RH(M)} \xrightarrow{K_9} \mathrm{R}\cdot \text{ or } \mathrm{P}\cdot \qquad [\mathrm{RO}_2\cdot][\mathrm{RH(M)}]K_9 \tag{27}$$

$$\mathrm{PO}_2\cdot + \mathrm{M} \xrightarrow{K_{10}} \mathrm{P}\cdot \qquad [\mathrm{PO}_2\cdot][\mathrm{M}]K_{10} \tag{28}$$

The change in initiator radical concentration [R·] is given by

$$\frac{\mathrm{d}[\mathrm{R}\cdot]}{\mathrm{d}t} = I_{\mathrm{abs}}\phi_{\mathrm{st}} - [\mathrm{R}\cdot][\mathrm{M}]K_1 - [\mathrm{R}\cdot][\mathrm{O}_2]K_2 - 2[\mathrm{R}\cdot]^2K_5 - [\mathrm{R}\cdot][\mathrm{RO}_2\cdot]K_7 + [\mathrm{RO}_2\cdot][\mathrm{RH(M)}]K_9 \tag{29}$$

The change in O_2 concentration is given by

$$\rho = \frac{-\mathrm{d}[\mathrm{O}_2]}{\mathrm{d}t} = [\mathrm{R}\cdot][\mathrm{O}_2]K_2 + [\mathrm{P}\cdot][\mathrm{O}_2]K_4 \tag{30}$$

The change in polymer radical concentration is given by

$$\frac{\mathrm{d}[\mathrm{P}\cdot]}{\mathrm{d}t} = [\mathrm{R}\cdot][\mathrm{M}]K_1 + [\mathrm{PO}_2\cdot][\mathrm{M}]K_{10} - [\mathrm{P}\cdot][\mathrm{O}_2]K_4 - 2[\mathrm{P}\cdot]^2K_6 - [\mathrm{P}\cdot][\mathrm{POO}\cdot]K_8 + [\mathrm{RO}_2\cdot][\mathrm{RH(M)}]K_9 \tag{31}$$

Assuming steady state conditions for $[\mathrm{RO}_2\cdot]$ leads to

$$0 = \frac{\mathrm{d}[\mathrm{RO}_2\cdot]}{\mathrm{d}t} = [\mathrm{R}\cdot][\mathrm{O}_2]K_2 - [\mathrm{R}\cdot][\mathrm{RO}_2\cdot]K_7 - [\mathrm{RO}_2\cdot][\mathrm{RH(M)}]K_9 \tag{32}$$

$$[\mathrm{RO}_2\cdot][\mathrm{RH(M)}]K_9 = [\mathrm{R}\cdot][\mathrm{O}_2]K_2 - [\mathrm{R}\cdot][\mathrm{RO}_2\cdot]K_7 \tag{33}$$

Substitution of eq 33 into eq 29 leads to

$$\frac{\mathrm{d}[\mathrm{R}\cdot]}{\mathrm{d}t} = I_{\mathrm{abs}}\phi_{\mathrm{st}} - [\mathrm{R}\cdot][\mathrm{M}]K_1 - 2[\mathrm{R}\cdot][\mathrm{RO}_2\cdot]K_7 - 2[\mathrm{R}\cdot]^2K_5 \tag{34}$$

Two sets of simplifying assumptions can be made to obtain an expression for the relationship between ρ and [DEABP]. In the first case it can be assumed that the primary radical (R·)-monomer reaction is extremely inhibited by oxygen. Therefore, $K_1 \ll K_7$ and K_5 and if $[\mathrm{R}\cdot] \gg [\mathrm{RO}_2\cdot]$ with the assumption of steady state conditions for [R·], the following expression for [R·] is obtained.

$$[\mathrm{R}\cdot] = (I_{\mathrm{abs}}\phi_{\mathrm{st}}/2K_5)^{1/2} \tag{35}$$

Assuming that $K_4 \ll K_2$ leads to

$$\rho = [\mathrm{O}_2]K_2(I_{\mathrm{abs}}\phi_{\mathrm{st}}/2K_5)^{1/2} \tag{36}$$

Expressed in terms of the photoinitiator concentration, the expression for ρ leads to

$$\rho = (I_0[\mathrm{DEABP}]\epsilon\phi_{\mathrm{st}}/2K_5)^{1/2}[\mathrm{O}_2]K_2 \tag{37}$$

In the second case monomer–initiator radical interaction as well as the polymer radical oxygen interaction is considered. If $K_9 \ll K_2$ and K_7 eq 32 leads to the following expression for $[\mathrm{RO}_2\cdot]$

$$[\mathrm{RO}_2\cdot] = [\mathrm{O}_2]K_2/K_7 \tag{38}$$

Then substituting eq 38 into eq 29 leads to

$$0 = \frac{\mathrm{d}[\mathrm{R}\cdot]}{\mathrm{d}t} = I_{\mathrm{abs}}\phi_{\mathrm{st}} - [\mathrm{R}\cdot]([\mathrm{M}]K_1 + 2[\mathrm{O}_2]K_2) - [\mathrm{R}\cdot]^2K_5 \tag{39}$$

Neglecting bimolecular termination (K_5) gives the final expression for [R·]

$$[\mathrm{R}\cdot] = I_{\mathrm{abs}}\phi_{\mathrm{st}/([\mathrm{M}]K1} + 2[\mathrm{O}_2]K_2) \tag{40}$$

Upon neglecting K_4, K_8, K_9, and K_{10} in eq 31 and assuming steady state conditions leads to the following expression for [P·]

$$[\mathrm{P}\cdot] = [I_{\mathrm{abs}}\phi_{\mathrm{st}}[\mathrm{M}]K_1/([\mathrm{M}]K_1 + 2[\mathrm{O}_2]K_2)2K_6]^{1/2} \tag{41}$$

Substitution of eq 40 and 41 into eq 3 leads to the final expression for ρ and

$$\rho = \frac{I_{\mathrm{abs}}\phi_{\mathrm{st}}[\mathrm{O}_2]K_2}{[\mathrm{M}]K_1 + 2[\mathrm{O}_2]K_2} + \left(\frac{I_{\mathrm{abs}}[\mathrm{M}]K_1}{([\mathrm{M}]K_1 + 2[\mathrm{O}_2]K_2)2K_6}\right)^{1/2}[\mathrm{O}_2]K_4 \tag{42}$$

A plot of log ρ vs. log [DEABP] is shown in Figure 5. The slope of the plot yields a value of 0.548 with a correlation coefficient of 0.972 for the plot. The initiator order of 0.548 indicates the predominance of the square root term in eq 42 for case 2 and agrees well with the theoretical half-order dependence of the initiator in eq 37 for case 1. Thus, the experimental data show plausibility of either set of assumptions made in case 1 or case 2.

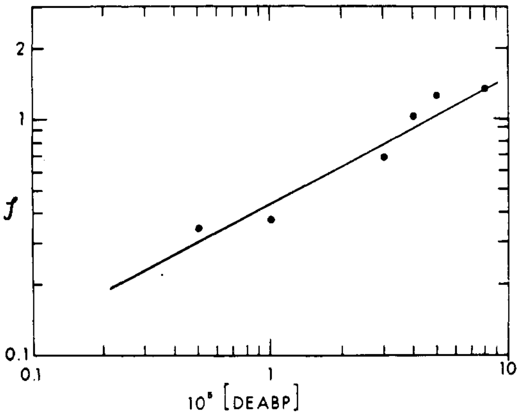

Figure 5. Log relative change in oxygen concentration (ρ) vs. log [DEABP].

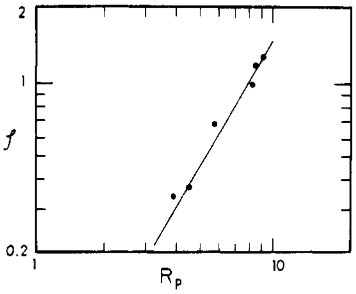

Figure 6. Plot of relative change in oxygen concentration (ρ) vs. rate of polymerization (R_p).

Now considering the polymer radical–oxygen termination reaction only as shown in eq 22, and neglecting K_2, eq 30 can be written as

$$\rho = [\mathrm{P}\cdot][\mathrm{O}_2]K_4 \tag{43}$$

In the ideal case of only the propagation reaction shown in eq 21

$$[\mathrm{P}\cdot] = R_{\mathrm{p}}/[\mathrm{M}]K_3 \tag{44}$$

and then

$$\rho = R_{\mathrm{p}}[\mathrm{O}_2]K_4/[\mathrm{M}]K_3 \tag{45}$$

A plot of ρ vs. R_p is linear as shown in Figure 6 and has a 0.98 correlation coefficient indicating agreement with the simplified theoretical expression in eq 45.

Figure 7 shows the composite GPC traces of the PMMA samples photopolymerized in the presence of nitrogen, air, and oxygen, respectively. It is seen that the polymers formed in nitrogen have the broadest molecular weight distributions. In our previous study[2a] these molecular weight distributions showed a polydispersity index of less than 2 indicating primary radical termination or chain transfer of the growing polymer radical with photoinitiator (radical) or photoproduct. In pure oxygen the molecular weight distributions were much narrower suggesting additional faster termination reactions competing with photochemically generated radicals or photoproducts observed under nitrogen atmosphere conditions.[10,11]

Aminoaromatic ketones can undergo electron transfer re-

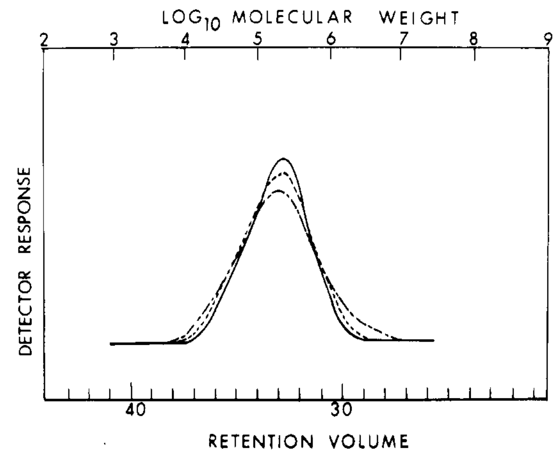

Figure 7. GPC curves for molecular weight distributions of photopolymerized MMA, [DEABP] = 4 × 10^{-5} M, in nitrogen (- -), air (- - -), and pure oxygen (—).

actions with other types of aromatic carbonyl compounds as shown in the following reaction sequence:

$$\mathrm{DEABP} \xrightarrow{h\nu} \mathrm{DEABP}^1 \xrightarrow{\phi_{st}} \mathrm{DEABP}^3 \qquad (46)$$

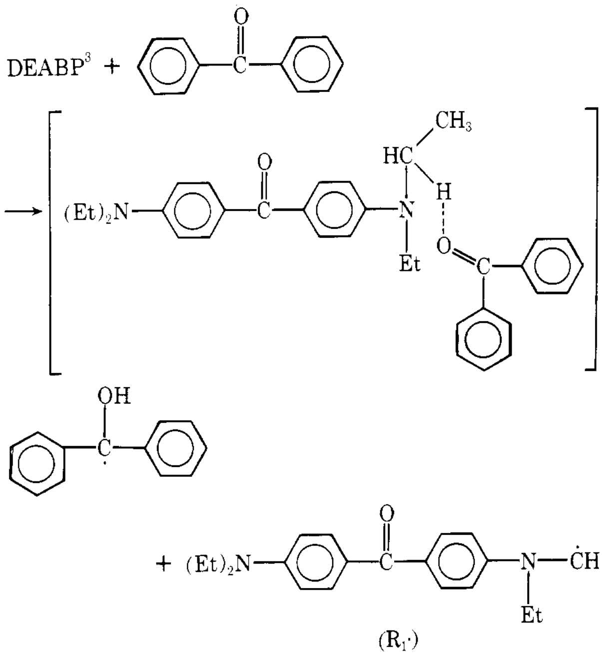

(47)

The triplet excited state of DEABP interacts with the ground state benzophenone resulting in electron transfer followed by proton transfer to give the ketyl radical and initiating radical R$_1$·.[12] Substituent effects on the aromatic carbonyl compounds (benzophenone and benzaldehyde derivatives) were studied with regard to their ability to effect changes in τ during the photopolymerization of MMA in air at constant DEABP concentrations.

The primary light absorbing species in these reactions is DEABP (λ_{max} 350 nm, $\epsilon \equiv 40{,}700$) and not the substituted benzophenone or benzaldehyde derivatives.[13,14] The results of these studies are shown in Figures 8 and 9 indicating electron withdrawing substituents facilitate rapid changes in the induction period (shorter time to reach steady rates of monomer conversion) while electron donating groups on the aromatic carbonyl derivatives tend to lengthen the induction period. The slope values are small but measurable indicating some sort of charge separation in the transition states. The electron-withdrawing groups could also facilitate the primary electron transfer mechanism during exciplex formation of the excited DEABP with aromatic carbonyl ground state molecules. The electron-withdrawing substituents on the aromatic carbonyl compounds showed less oxygen sensitivity and slightly faster rates of photopolymerization than the electron-donating substituents.

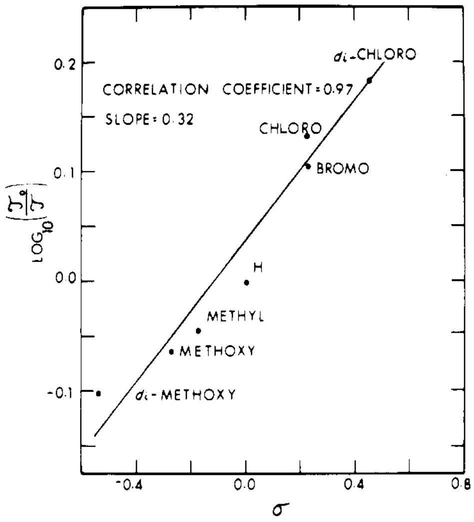

Figure 8. Correlation of Hammett σ and length of induction period (τ) for benzophenone (τ_0) and parasubstituted benzophenones (τ) with a constant [DEABP] = 2 × 10^{-4} M; [substituted and unsubstituted benzophenones] = 6 × 10^{-4} M. Photopolymerization of MMA in air at 30 °C.

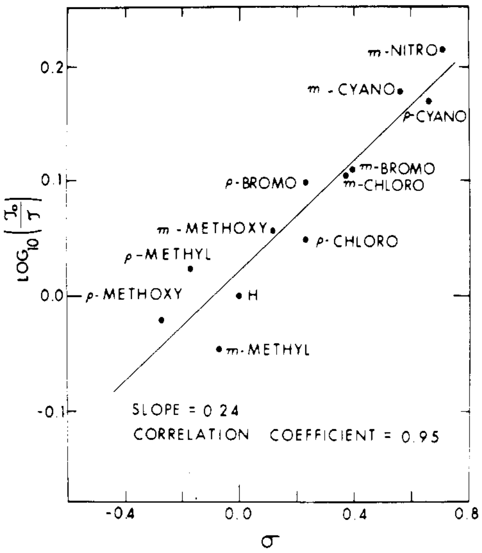

Figure 9. Substituent effect on the length of induction period (τ) for the photopolymerization of MMA in air with benzaldehyde (τ_0) and substituted benzaldehydes (τ) at a constant [DEABP] = 2 × 10^{-4} M, [aldehyde] = 6 × 10^{-4} M.

In conclusion, aminoaromatic ketones can be shown to have varied mechanistic photochemical pathways for production of a free radical initiating species. These compounds also have measurable concentration and molecular structural effects on physical property relationships.

Acknowledgments. Part of this work performed by A. Gallopo was supported by a National Science Foundation "Faculty Research Participation" grant having Proposal/Grant No. SER-76-04704.

References and Notes

(1) (a) Address correspondence to this author at Battelle Columbus Laboratories, Columbus, Ohio 43201; (b) Montclair State College.
(2) (a) V. D. McGinniss, T. Provder, C. Kuo, and A. Gallopo, *Macromolecules*,

preceding paper in this issue; (b) D. Phillips, *J. Oil Colour Chem. Assoc.*, **59**, 202 (1976).
(3) T. Kodaira, K. Hayashi, and T. Ohnishi, *Polym. J.*, **4**, 1 (1973).
(4) T. Kodaira and K. Hayashi, *J. Polym. Sci., Polym. Lett.*, **9**, 907 (1971).
(5) F. Wilkinson, *Adv. Photochem.*, 3 (1964).
(6) P. Suppan, *J. Chem. Soc., Faraday Trans. 1*, **71 (3)**, 539 (1975).
(7) D. I. Schuster, M. D. Goldstein, and P. Bane, *J. Am. Chem. Soc.*, **99**, 187 (1977).
(8) P. D. Bartlett and H. Kwart, *J. Am. Chem. Soc.*, **72**, 1051 (1950).
(9) L. Reich and S. S. Stivala, "Elements of Polymer Degradation", McGraw-Hill, New York, N.Y., 1971.
(10) C. H. Bamford et al., "The Kinetics of Vinyl Polymerization by Radical Mechanisms", Butterworths, London, 1958.
(11) G. Gee and H. W. Melville, *Trans. Faraday Soc.*, **44**, 240 (1944).
(12) C. C. Wamser et al., *J. Am. Chem. Soc.*, **92**, 6362 (1970).
(13) V. D. McGinniss, *ACS Symp. Ser.* **No. 25**, 135 (1976).
(14) S. L. Murov, "Handbook of Photochemistry", Marcel Dekker, New York, N.Y., 1973.

The Effect of Side-Chain Branching on the Theoretically Predicted Conformational Space Available to Amino Acid Residues

Yvonne Paterson and Sydney J. Leach*

Russell Grimwade School of Biochemistry, University of Melbourne, Parkville, Victoria, 3052, Australia.

Received July 11, 1977

ABSTRACT: This study uses the most recently refined conformational energy parameters to define the conformational space available to both the backbone and side chains of the *N*-acetyl-*N'*-methylamide derivatives of alanine, β-methylalanine, valine, and β-methylvaline. The conformational space is described in terms of both conformational energy values and statistical percentage probabilities for 10° increments of ϕ and ψ and for different rotameric states of the side-chain torsion angles. Of the various regions of the (ϕ,ψ) map, the area surrounding the C_7^{eq} conformation is the most favored overall for alanine, β-methylalanine, and valine, whereas that containing the extended conformational energy minimum is the most probable for β-methylvaline. For both the valine and β-methylalanine residues the trans rotameric state for the C^α–C^β bond strongly predominates (88 and 62% probabilities, respectively).

A central tenet in the prediction of the conformations of larger peptides is the belief that the conformational space available to the peptide backbone immediately adjacent to any residue is largely governed by the nature and conformations of the latter's side chain. Thus, there has been increasing interest in the experimental conformational analysis of the side chains of biologically active peptides which has been facilitated by the application of high-resolution techniques such as NMR.[1,2] Conformational energy calculations have been used to predict the most probable conformation of a peptide where there is more than one conformation consistent with the experimental data.[3,4]

The number of possible side-chain conformations for most naturally occurring amino acids is sufficiently large to preclude a total search of the conformational space available to the backbone, exceptions being glycine, alanine, and proline. Attention has therefore been focused on establishing their minimum energy conformations.[5,6] Amino acids with short side chains, branched at the C^β atom, are small enough to allow an exhaustive description of the total space available to such amino-acid residues.

The side-chain conformations of these amino acids are uniquely defined by the value of the variable side-chain torsion angle χ^1. Only the three values which "stagger" the positions of the substituents at either end of the C^α–C^β bond need be considered. These values are 180 ± 30°, 60 ± 30°, and −60 ± 30°, and the positions they define are designated trans, gauche$^+$, and gauche$^-$, respectively. Valine and threonine are the only amino acids that occur in proteins for which the above simplifications apply. However, β-methylalanine, an amino acid that is frequently used in synthetic analogues of biologically active peptides,[7,8] can also be treated in this way.

Substituting a third methyl group onto the C^β carbon atom of valine, to give β-methylvaline, gives a symmetric side chain for which only one value of χ^1 need be considered, namely that in which the three C^γ methyl groups are staggered with respect to the backbone bonds. β-Methylvaline is thus an interesting model for steric restrictions imposed by bulky side chains on the backbone conformations of the polypeptide chain.

The purpose of the present study is to explore the total conformational space available to β-methylalanine, valine, and β-methylvaline using a recently refined set of empirical potentials and parameters.[9]

Methods

Nomenclature and Abbreviations. The amino acid L-2-aminobutanoic acid has been given the trivial name β-methylalanine in this paper. It is also known as α-amino-*n*-butyric acid.[17] L-2-amino-(3,3)-dimethylbutanoic acid, which has been referred to as *tert*-leucine by other workers,[22] is called β-methylvaline in this study. Unless explicitly stated, all amino acid residues are considered in their L configuration. All other nomenclature and conventions used are those recommended by the IUPAC-IUB Commission.[10]

Energy Calculations and Minimizations. Conformational energies were calculated using ECEPP[11] (Empirical Conformational Energy Program for Peptides) with a Cyber 73 computer. This program was developed in the Department of Chemistry at Cornell University and uses the empirical potential energy functions and energy parameters described by Momany et al.[9] It was modified to be compatible with the Cyber system. The total conformational energy of the molecules is calculated as the sum of the electrostatic, nonbonded, and torsional energy components from interatomic interactions. Hydrogen atoms are considered explicitly and the hydrogen-bond energy is included in the nonbonded energy component.[9]

Energy minimizations were performed using ECEPP in conjunction with a function-minimizing subroutine.[12] Minimization was terminated when the conformational energy changed by less than 0.01 kcal/mol between successive calculations.